Case report

Primary hepatic neuroendocrine tumor: gadoxetic acid (Gd-EOB-DTPA)-enhanced magnetic resonance imaging

Soo-heui Baek[1], Jung-Hee Yoon[1] and Kwan-woo Kim[2]

[1]Department of Radiology; [2]Department of Surgery, Haeundae Paik Hospital, Inje University College of Medicine, Busan, Republic of Korea
Correspondence to: Jung-Hee Yoon. Email: radyjh@hanmail.net

Abstract

We present a case of a 71-year-old man with prostate cancer who had no prior underlying liver disease. During metastatic evaluation, a solid mass in the liver was identified by computed tomography and ultrasound. Gadoxetic acid (Gd-EOB-DTPA)-enhanced magnetic resonance imaging demonstrated a well-defined, peripheral enhancing hepatic mass containing small cystic component. This lesion was diagnosed as hepatic neuroendocrine tumor. Primary neuroendocrine tumors of the liver are extremely rare. This case is interesting because of the rarity of this neoplasm and the unique radiologic findings despite its small size. Reviews of previously reported cases in the literature are also presented.

Neuroendocrine tumors (NETs) mainly arise in the broncho-pulmonary or gastrointestinal tract, but can occur in almost any organ. NETs have varied malignant potential depending on the site of their origin (1). Primary hepatic NETs are extremely rare, when a NET is found in the liver, it must be treated with great care to exclude metastasis from extrahepatic primary site, as that is a much more common occurrence (2). The first reported case was documented by Edmondson in 1958 (3). Thereafter, only fewer than 60 cases of primary hepatic NET have been reported in the English literatures (4) and they mainly focus on computed tomography (CT) findings. To the best of our knowledge, there is no report of the primary hepatic NET focusing on magnetic resonance imaging (MRI) using hepatobiliary-specific contrast agent.

Case report

A 71-year-old man presented to our outpatient clinic 3 years ago for the evaluation of metastasis with documented prostate cancer, which was diagnosed elsewhere. The patient reported no clinical symptoms, such as flushing, fever, or abdominal pain. A physical examination revealed no abnormal findings. The results of other laboratory evaluations, including liver tests and blood level of tumor markers (i.e. alpha-fetoprotein, CA-19–9, and carcinoembryonic

antigen), were within normal limits. An ultrasound examination revealed a heterogeneous mixed echoic solid mass in the left lateral segment of the liver that was approximately 3.7 cm in maximal diameter (Fig. 1). Abdominal multidetector CT revealed a well-circumscribed, heterogeneous, and hypodense mass, with mild peripheral constant enhancement during the arterial, portal, and equilibrium phases (Fig. 2). The liver background was not cirrhotic. MR images (Fig. 3) were obtained with a 1.5 T unit using a liver-specific contrast agent (gadoxetic acid disodium [Gd-EOB-DTPA], Primovist®, Bayer Healthcare, Berlin, Germany). On T2-weighted fast spin-echo MR (TR/TE, 3646.3/107.0) and diffusion images (diffusion b-factor, 800), the mass was mainly with mild high signal intensity correlated with normal liver parenchyma with several foci of hyperintense foci. This mass demonstrated hypointensity on T1-weighted gradient echo images (TR/TE, 3.6/1.4), and the previously highly hyperintense foci on T2-weighted images showed also slightly hyperintense on T1-weighted image, suggesting a hemorrhagic component. Gadoxetic acid-enhanced T1-weighted MR images demonstrated peripheral enhancement of the solid tumor portion on early arterial phase, contrast wash-out pattern on portal venous phase and definite defect on 20 min delayed hepatobiliary phase. The patient underwent ultrasound-guided biopsy of the hepatic mass, and histology suggested a malignant neoplasm that originated from a neuroendocrine cell

(well-differentiated neuroendocrine carcinoma, Grade 2). After a meticulous examination for the primary origin, including positron emission tomography-computed tomography (^{18}F-FDG-PET/CT), colonoscopy, gastroscopy, and chest CT, there was no evidence of a primary focus. On ^{18}F-FDG-PET/CT, there was no definite increase of glucose metabolism in the hepatic tumor (Fig. 4). Although grade 2 neuroendocrine tumors demonstrate slow growth, surgical resection is the treatment of choice. Based on this pathologic
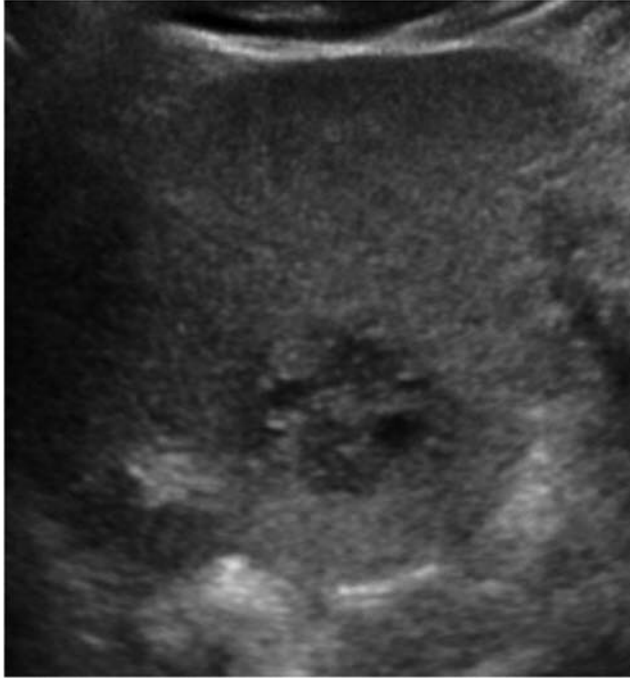
diagnosis, a left hemihepatectomy was performed. During the operation, no evidence of ascites or liver cirrhosis was found. The gross features of the tumor appeared approximately 3.3 cm in size with well-defined margins and a pink-yellowish appearance. The tumor consisted of multiple small hemorrhagic vascular lakes with old blood. Microscopic examination revealed that the neoplasm comprised cell atypia and mitotic activity (8/10 HPF, Fig. 5). Small-intermediate-sized tumor cells demonstrated uniformly round nuclei with abundant cytoplasm and vesicular nuclei chromatin. Immunohistochemical studies were performed (Fig. 5), and the tumor cells were strongly positive for the neuroendocrine marker synaptophysin, focally positive for neural adhesion molecule (CD56)/chromogranin and negative for cytokeratin 7 (a marker for cholangiocarcinoma). Ki-67 proliferative index is positive in 5% of cells. Microscopic and immunohistochemical findings were compatible with a well-differentiated G2 neuroendocrine carcinoma based on the WHO 2010 criteria (5). Based on this finding, we performed a more thorough study to rule out the possibility that the liver tumor was a metastatic NET during the 3-year follow-up period. This work-up included multiple upper gastrointestinal endoscopies, colonoscopy, abdominal ultrasound examination, chest and abdominal CT scans, ^{123}I-MIBG scan, and ^{123}I-Octreotide SPECT-CT. All imaging findings were normal, except mild duodenitis. Thus, we concluded that the final diagnosis in this case was primary hepatic NET.

Fig. 1 Ultrasound examination demonstrates a heterogeneously mixed echoic solid mass in the left lateral segment of the liver

Discussion

NETs consist of a heterogeneous group of malignancies with various clinical presentations and growth rates. The overall incidence of carcinoid tumors in the United States

Fig. 2 MDCT scan, axial images. A well-circumscribed, heterogeneous, and hypodense liver mass (white arrow): arterial (left)/equilibrium (right). The lesions demonstrate mild peripheral enhancement, and suspected intratumoral cystic foci are delineated. CT scan demonstrating that the background liver is not cirrhotic
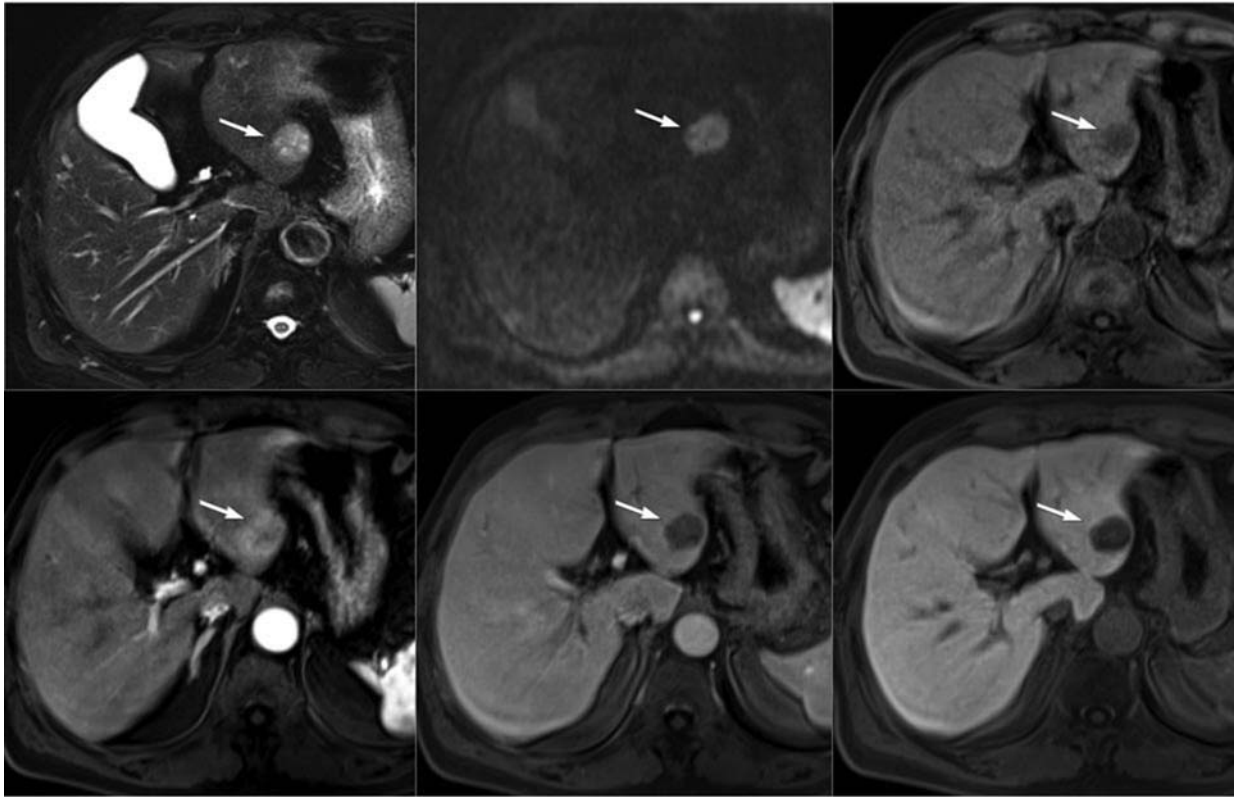
Fig. 3 MR images. A T2-weighted axial image (top left): a well-circumscribed, subtly hyperintense nodule (arrow) is associated with the normal liver parenchyma and contains several hyperintense foci; Diffusion b = 800 (top middle): homogeneously hyperintense; Precontrast T1-weighted image (top right): the main lesion demonstrates hypointensity, and the foci on T2-weighted image are visualized with subtle hyperintensity (arrow); On gadoxetic acid (Gd-EOB-DTPA)-enhanced MR images, the lesion demonstrates peripheral enhancement on the arterial phase (bottom left) and a definite contrast wash-out pattern with peripheral rim enhancement on the portal venous phase (bottom middle) and a 20-min delayed phase (bottom right). Previously noted cystic lesions are suspected to have a hemorrhagic component on the basis of the MR signal
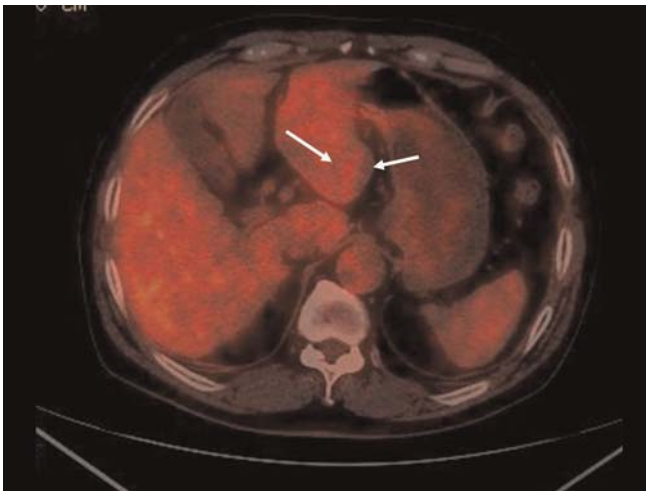

Fig. 4 ^{18}F-FDG-PET/CT scan demonstrates a mild contour building hepatic mass in the left lobe lateral segment without definite increased uptake (arrows)

has been estimated to be 1–2 cases per 100,000 people (6). Because of many carcinoid tumors are indolent, their true incidence may be higher. The largest group is the gastro-enteropancreatic NETs that account for 2% of all gastro-intestinal tumors (7). A classification system (World Health Organization) was established in 2000 and recently updated in 2010, differentiating between the terms NET and neuroendocrine carcinoma (5). Proliferation index (Ki-67, MIB-1), angioinvasion, and mitoses are important factors in this classification. Thus, tumors are divided into well-differentiated NETs (<2 cm in size, <2% Ki-67 index), well-differentiated neuroendocrine carcinomas (>2 cm in size, >2% Ki-67 index, or angioinvasive), and poorly differentiated neuroendocrine carcinoma (Ki-67 index > 20%).

Primary hepatic NETs are typically slow-growing and non-functional in most cases, incidentally detected, commonly occur in patients aged >50 years and are slightly more frequent in women (8).

The histogenesis of primary hepatic NETs has not been established. One theory is that primary hepatic NETs are presumably derived from scattered neuroendocrine cells in the intrahepatic biliary epithelium. Another theory is that chronic inflammation in the biliary system may predispose an individual to a NET by initiating intestinal metaplasia (4). However, because no significantly different imaging findings were found between primary and metastatic NETs, we speculate that metastases and primary hepatic NETs likely display the same vascular pattern and tissue characteristics. Furthermore, liver and lymph nodes are the most common sites of metastasis from midgut NETs (1).

In our case, we performed a thorough investigation to exclude the possibility of a metastatic NET, but we could
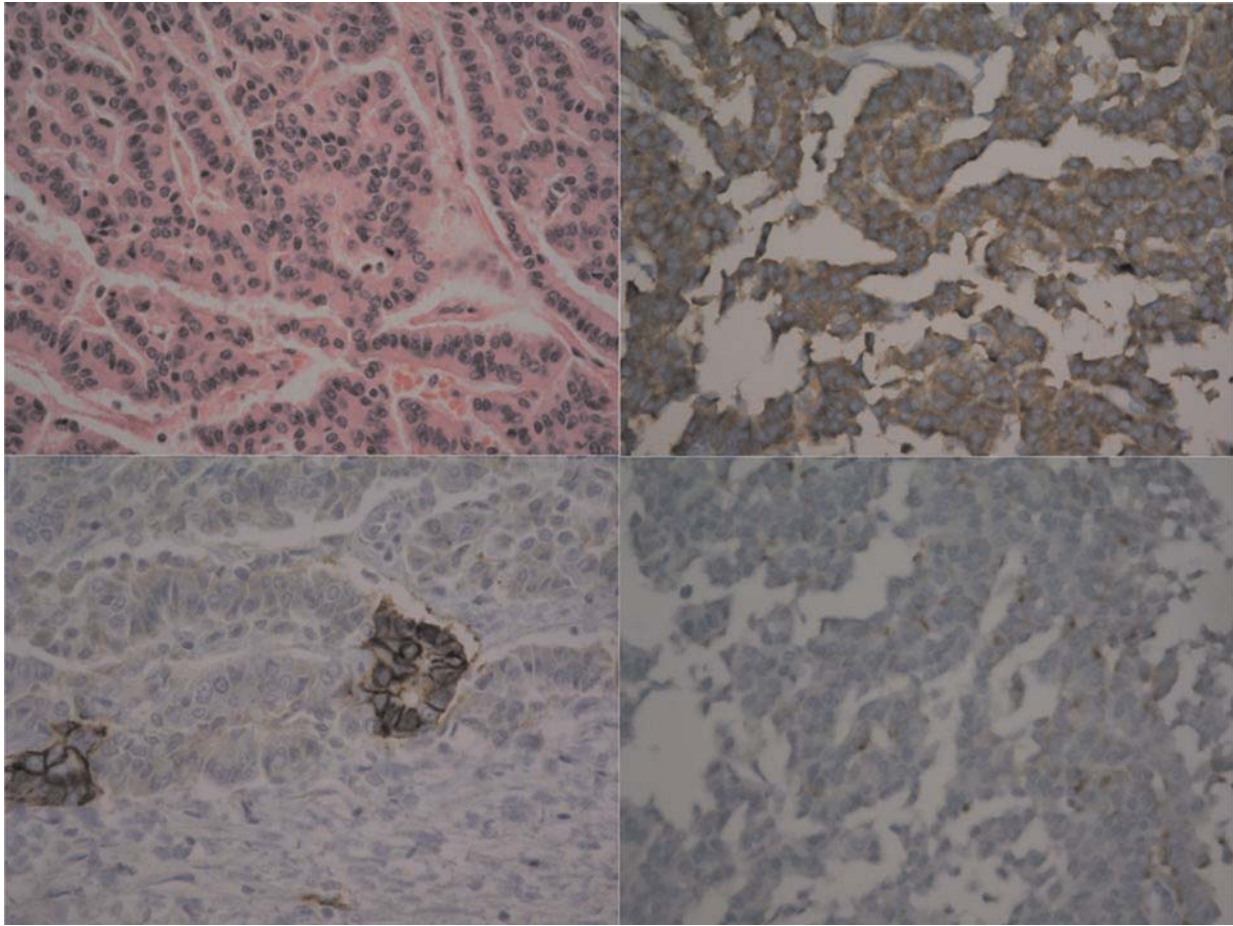
Fig. 5 Microscopic findings of a primary hepatic neuroendocrine tumor. High-power field (200×) (top left): small to intermediately sized uniform population of tumor cells demonstrating abundant cytoplasm with round smooth contour nuclei and vesicular nuclear chromatin. Immunohistologic synaptophysin staining (top right) in positive tumor cells. Staining for CD56 (bottom left)/chromogranin (bottom right) in focal positive neuroendocrine cells

not identify any primary intestinal or bronchogenic tumors. A definitive diagnosis for a primary hepatic NET is difficult, as the radiologic findings can resemble HCC, metastasis, focal nodular hyperplasia, hepatic adenoma, and cholangiocarcinoma. The differential diagnosis of primary hepatic NETs from the more common forms of this disease (i.e. HCC and metastasis) is important because NETs are associated with a more indolent course and require different management. Based on these radiologic findings, the possibility of hypervascular metastasis and small HCC occurring in the normal background should be suggested. It has been reported that some hypervascular metastasis with rapid growth may be accompanied by a cystic or hemorrhagic change and HCC in non-cirrhotic livers in up to 40% of HCC patients (9). This case was a single hypervascular hepatic mass in the normal background liver (no chronic hepatitis B or C or alcoholic) and contained intratumoral tiny cystic spaces, which are not common findings in small nodular HCC's, although this mass shows similar enhancement pattern mimicking HCC. This unique findings are well demonstrated on gadoxetic acid-enhanced MRI because of excellent tissue contrast and spatial resolution of essential MRI and highly sensitive for the detection of focal liver lesion at the delayed hepatobiliary phase due to high tissue contrast between strong parenchymal

enhancement and focal liver lesion and highly specific for characterization of focal liver lesion using dynamic contrast imaging. Small hepatic NETs (<2 cm) are homogeneously enhanced, while large hepatic NETs are peripherally enhanced in the arterial phase. Most lesions demonstrate delayed contrast wash-out due to hypervascularity and central necrosis, but progressive enhancement has also been reported due to proliferative fibrous tissue inside the lesion (10). Most lesions usually present with hypointensity on T1-weighted and hyperintensity on T2-weighted MR images because of their complex cystic nature (11). The image modality of choice for NET staging is CT, MRI, SPECT/CT, and PET/CT. In particular, the latter two modalities in combination with sensitive NET tracers are reported to have high sensitivity (12). However, only NETs with high proliferative activity and low differentiation may demonstrate increased ^{18}F-FDG uptake (13). Currently, ^{123}I-MIBG or somatostatin receptor scintigraphy such as ^{123}I-Octreotide scintigraphy is the gold standard for NET staging (14).

In our case, there was no abnormality during the preoperative evaluation of ^{18}F-FDG-PET/CT and postoperative follow-up of ^{123}I-MIBG scan and ^{123}I-Octreotide SPECT-CT, but still a carcinoma of unknown primary lesion may be considered as a differential diagnosis. The rarity of

primary hepatic NET makes it difficult to suspect and diagnose preoperatively; thus, the patient's clinical history is often helpful in these cases. A final primary hepatic NET diagnosis should be confirmed by pathological and immunohistochemical examinations. Neoplastic cells usually stain positive for endocrine markers, including chromogranin, synaptophysin, and neuron-specific enolase. The main treatment for primary hepatic NETs is liver resection, and a 74% postoperative 5-year survival rate and an 18% recurrence rate have been reported (9). Primary hepatic NETs are interesting entities that if correctly diagnosed and treated, may achieve favorable long-term results.

In conclusion, a rare primary hepatic NET with unique radiologic findings is presented with a focus on dynamic and hepatobiliary-specific contrast MRI and histopathologic findings with immunochemistry.

REFERENCES

1 Scarsbrook AF, Ganeshan A, Statham J, *et al.* Anatomic and functional imaging of metastatic carcinoid tumors. *Radiographics* 2007;**27**:455–76

2 Iwao M, Nakamuta M, Enjoji M, *et al.* Primary hepatic carcinoid tumor: case report and review of 53 cases. *Med Sci Monit* 2001;**7**:746–50

3 Kehagias D, Moulopoulos L, Smirniotis V, *et al.* Imaging findings in primary carcinoid tumour of the liver with gastrin production. *Br J Radiol* 1999;**72**:207–9

4 Touloumis Z, Delis SG, Triantopoulou C, *et al.* Primary hepatic carcinoid; a diagnostic dilemma: a case report. *Cases J* 2008;**1**:314

5 Luttqes J. [What's new? The 2010 WHO classification for tumours of the pancreas]. *Pathologe* 2011;**32**(Suppl. 2):332–6

6 Modlin IM, Sandor A. An analysis of 8305 cases of carcinoid tumors. *Cancer* 1997;**79**:813–29

7 Wallace S, Ajani JA, Charnsangavei C, *et al.* Carcinoid tumors: imaging procedures and interventional radiology. *World J Surg* 1996;**20**:147–56

8 Miura K, Shirasawa H. Primary carcinoid tumor of the liver. *Am J Clin Pathol* 1988;**89**:561–4

9 Brancatelli G, Federle MP, Grazioli L, *et al.* Hepatocellular carcinoma in Noncirrhotic liver: CT, clinical, and pathologic findings in 39 U.S residents. *Radiology* 2002;**222**:89–94

10 Takayasu K, Muramatsu Y, Sakamoto M, *et al.* Findings in primary hepatic carcinoid tumor: US, CT, MRI and angiography. *J Comput Assist Tomogr* 1992;**16**:99–102

11 Bader TR, Semelka RC, Chiu VC, *et al.* MRI of carcinoid tumors: spectrum of appearances in the gastrointestinal tract and liver. *J Magn Reson Imaging* 2001;**14**:261–9

12 Haug AR, Cindea-Drimus R, Auernhammer CJ, *et al.* The role of 68Ga-DOTATATE PET/CT in suspected neuroendocrine tumors. *J Nucl Med* 2012;**53**:1686–92

13 Sundin A, Eriksson B, Bergstrom M, *et al.* PET in the diagnosis of neuroendocrine tumors. *Ann NY Acad Sci* 2004;**1014**:246–57

14 Rufini V, Calcagni ML, Baum RP. Imaging of neuroendocrine tumors. *Semin Nucl Med* 2006;**36**:228–47